Ultra-Wide Band Frequency Selective Surface: design and experimental verification of performances for wide incident angle

Ultra-Wide Band Frequency Selective Surface: design and experimental verification of performances for wide incident angle

Andrei-Marius Silaghi
Dept. of Measurements and Optical Electronics
Politehnica University Timisoara
Timisoara, Romania
andrei.silaghi@upt.ro

Aldo De Sabata
Dept. of Measurements and Optical Electronics
Politehnica University Timisoara
Timisoara, Romania
aldo.de-sabata@upt.ro

Ladislau Matekovits
Dept. of Electronics and Telecommunications
Politecnico di Torino, Torino, Italy,
Istituto di Elettronica e di Ingegneria dell'Informazione e delle Telecomunicazioni,
National Research Council of Italy, 10129 Turin, Italy,
Politehnica University Timisoara, Romania,
ladislau.matekovits@polito.it

Adrian-Petru Buta
Dept. of Measurements and Optical Electronics
Politehnica University Timisoara
Timisoara, Romania
adrianbutap@gmail.com

***Abstract*—In the established UWB frequency range, for spatial filtering purposes a frequency selective surface is presented, simulated results showing a very large stopband between 1.78-14.32 GHz. Thus, strong polarization insensitivity is obtained with the structure and 45º angular stability for the pair: Transverse Magnetic (TM) and Transverse Electric (TE) incidence, respectively. Electromagnetic simulation was used to evaluate the performances of the structure, considering a 1.6 mm thick FR4 substrate with a 15 mm square-shaped unit cell edge. In an anechoic chamber, tests revealed an excellent match between simulation and experimental data, as well as proper device operation.**

Keywords—FSS, UWB, spatial band-stop filter, practical validation.

I. INTRODUCTION

In the last decade, frequency selective surfaces (FSSs) fabricated on single-layer or stacked printed circuit boards (PCBs) [1] have been used as absorbers, artificial magnetic conductors, polarizers, screens and spatial filters and shields, among other things [2].

There has been a surge in interest in FSS applications as spatial filters, shields, and screens, with the introduction and rapid expansion of wireless communications systems in the last couple of decades. Screens can be used to shield some places, such as buildings and rooms, from electromagnetic radiation in certain frequency bands while leaving other frequency bands undisturbed. By integrating electronic equipment and high-frequency circuits into specifically constructed boxes with patterned walls, they can be insulated in certain frequency bands [2].

Some studies have used FSSs to apply spatial filtering in across a number of regulated wireless transmission spectrum bands.

For example, filtering in GSM bands was tackled in [3], [4], [5], whilst WiMAX and WLAN were approached in [4], [6], and [7]. Experimental prototypes on FR4 substrates were created with dimensions of 4x4 elements [3], 27x25.7 mm^2 [4], 13x10 unit cells [7], dimensions of 20x20 cm^2 [8]. Stable frequency response was obtained up to the following angles of incidence: 30º [9], 40º [8], 45º [3], [7], [4] and 60º [5].

The advancement of wireless technologies has also sparked interest in wide-band solutions research. An early design (which is made up of rings and cross dipoles on opposing parts of an FR-4 substrate having one layer of metal) has been reported in [10] providing a broad stopband between 6.5-14 GHz (7.5 GHz) in the X and Ka bands.

To obtain a tunable FSS, a structure made up varactor diodes that connect periodic designs of metallic loops in circle form has been introduced in [11]. With a rectangular unit cell of 12 mm in size, and according to the voltage of the diodes, the structure presented a 1.28 GHz delimited stopband, having a working frequency ranged from 0.54 GHz to 2.50 GHz.

An FSS having two distant layers with distinct transmission zeros, as well as a design of incurved cross dipoles, was explored in [12]. Numerical simulations and measurements were undergone for the aforementioned FSS exhibiting X band filtering.

In paper [13] the authors described a single-layer, one-sided method presenting in the frequency range 2.72-13 GHz a stopband with large extent. This solution which can be used as a reflector to improve the gain of UWB antennas, presented an angular stability of 80 degrees.

Finally, in [14] another single layer FSS is introduced, this time on the opposing sides of a FR4 substrate (having a thickness of 1.6mm). The stopband, designed with parallel component patches, reports angular stability of 45º and is obtained between 3.1 GHz and 13.3 GHz.

An FSS with a very large stopband is presented in this study, with the purpose of screening electromagnetic waves in the specified Ultra-Wideband (UWB) frequency domain. The design includes a stopband that is larger than the planned one (UWB normally extends from 3.1 GHz to 10.6 GHz) to ensure optimal operation (between 1.78 and 14.32 GHz, a -10 dB stopband is achieved, covering a 12.54 GHz wide bandwidth.).

The method is implemented on a FR4 substrate, which: is not so expensive, has two faces, one layer and is having a bigger stopband than those reported in recently published publications. The unit cell is 15x15 mm^2 in size. Experiments on a board having a number of unit cells equal to 30 × 30 were used to successfully verify the results of the numerical simulations.

The following parts of our article are presented next. In the next section, we have the description of the proposed solution and the presentation of the electromagnetic simulation results (used to evaluate the correct behavior). Parametric studies are also undergone in Section II, whilst experimental results are reported in Section III. The last section is dedicated to wrapping up the conclusions of the paper.

II. Presentation Of The Structure Solution

A. Initial simulations

Our intended periodic surface, having a unit cell with sizes of d_x=15 mm and d_y=15 mm and having metallization across the two faces of the used FR 4 substrate, is firstly depicted in Fig.1. The used substrate has the following parameters: a thickness st=1.6 mm, ε_r=4.3 and tanδ = 0.025.

The top side of the unit cell, which is a metallic structure, will be further referred as Face 1 (only this face is represented in Fig. 1). This pattern is made up of nine squares, all of them having margins of length L_1=2 mm, and being connected along their symmetry axes by lines of thickness w_1=0.4 mm. The structure is surrounded by a square ring of external length L_2=14.9 mm (calculated as the difference between d_x and d-equal to 0.1 mm, represents the distance between parallel rings within adjacent unit cells). This structure is a modified version of the one proposed earlier by the authors in [2].

By means of the simulation tool [15], firstly, the structure was tested with the E field being parallel to the d_y edge of the unit cell from Fig. 1, in a scenario known as TE polarization. Due to the symmetry of the unit cell structure, TM polarization produces the same results in normal incidence [2].

The transmittance is visible in Fig. 2 (with only Face 1 present). This first result plot indicates the apparition between 1.87 GHz and 9.58 GHz, of an extended -10 dB stop-band. It covers a large bandwidth of 7.71 GHz. Next, Face 2 (visible in Fig. 3) contains four metallic rectangles, of edge L_{sq}=4.4 mm, and one empty rectangle, located in the middle of the unit cell, having an edge L_3=4.5 mm.

Fig. 4 reveals the result with only Face 2 of the structure present: a first -10 dB stopband between 3.7 and 8.5 GHz and a second one between 13.46 and 13.86 GHz. In Fig. 5 one can see the 3D CAD model of the entire unit cell (with both faces present in simulation), the substrate being eliminated so that the entire metallization can now be visualized from both sides of the dielectric support.

A very wide -10 dB stop-band occurs between 1.78 GHz and 14.32 GHz, covering a 12.54 GHz broad bandwidth, as a result of the interaction of the two faces (Fig. 6). As a consequence, the proposed periodic structure functions as a band-stop filter with an ultra-wide bandwidth.

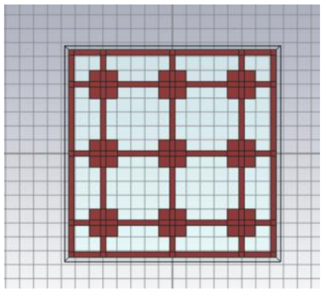

Fig. 1. Face 1 of the structure.

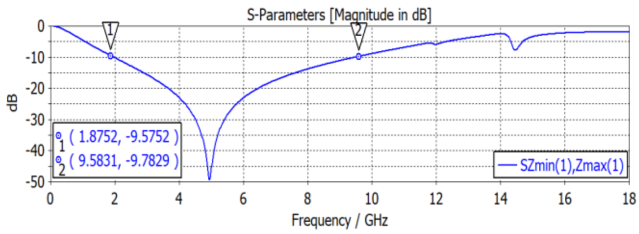

Fig. 2. Results for Fig. 1.

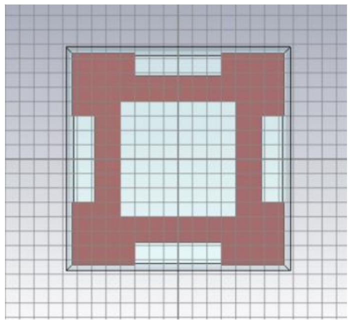

Fig. 3. Face 2 of the structure.

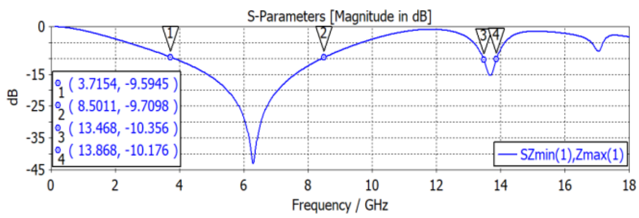

Fig. 4. Results for Fig.3.

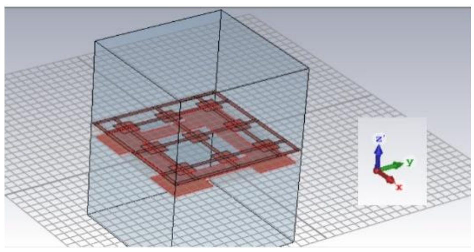

Fig. 5. Initial structure with both faces.

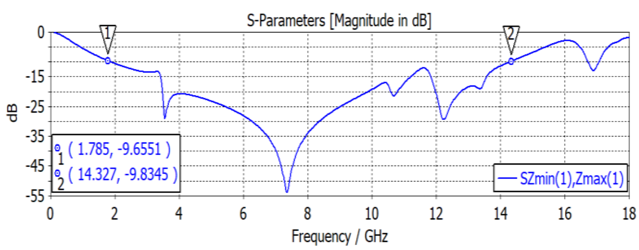

Fig. 6. Results for Fig. 5.

B. *Parametric studies*

The structure from Fig. 5 was subjected to a parametric investigation namely the variation of thickness of the FR4 substrate. Within the proposed solution, the length of the wave path is changed when the substrate thickness is modified, and this has an impact on the frequency response [16].

As shown in Fig. 7, the notches and the wide-band can be changed in frequency by adjusting this parameter from 0.8 to 2.4 mm for the FSS having the unit cell shown in Fig. 5. The wideband is slightly enhanced by reducing the substrate thickness.

Another parametric investigation on the structure from Fig. 5 was done to examine the sensitivity of an electromagnetic plane wave with regard to its incidence angle. Only the modification of the transmission coefficient with the colatitude angle has been considered due to the structures symmetry.

The results of the parametric change of the colatitude angle (theta) for the TE scenario are shown in Fig. 8. In 5 values, this parameter was changed from 0 to 60º. In TE mode, consistency for the wide band can be noticed up to 45º.

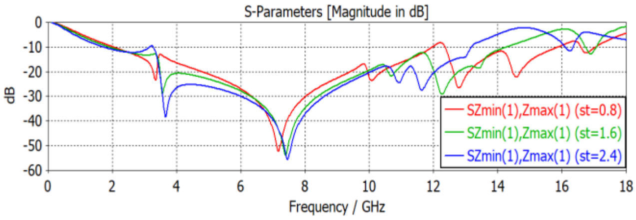

Fig. 7. Parametric study st for Fig. 5.

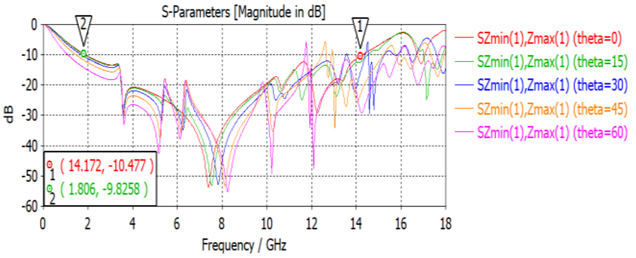

Fig. 8. Results of the parametric study for incidence angle (TE case).

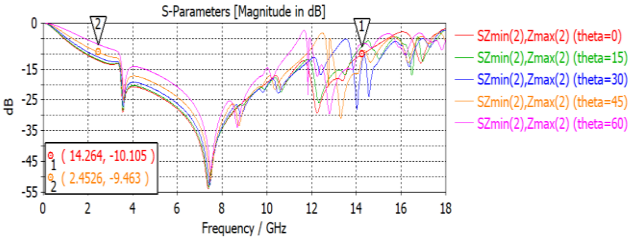

Fig. 9. Results of the parametric study for incidence angle (TM case).

III. Experimental Validation

The planned periodic structure (with a substrate thickness of 1.6mm) was created as a printed circuit board (PCB) prototype of FR4 type, with 30 unit cells in each of the two orthogonal axes and a total length of 450 x 450 mm^2. In Fig. 10, a snapshot of the prototypes Face 1 is shown. Measurements were made in an anechoic room, as releaved in Fig. 11, using the substitution method described in [2].

Fig. 12 shows the measured transmittance for TE incidence for colatitude theta between 0 and 45º. Because the effective aperture for incident waves reduces by 50% when compared to normal incidence, measurements have been limited to a 45º angle of incidence. Fig. 13 depicts the same curves but for TM incidence.

This combination of results is sufficient for assessing the variation of the transmittance at oblique incidence due to the symmetry of the metal design in the unit cell.

The results of simulation and measurements are in good agreement, according to the data exhibited previously. There are some small variations in the transmittace results that are caused by the following: tolerances in the metalization, variations in the geometry and imperfection in the PCBs dielectric, and by higher order modes which are launched as surface waves and can radiate when they reach the PCBs limits [2].

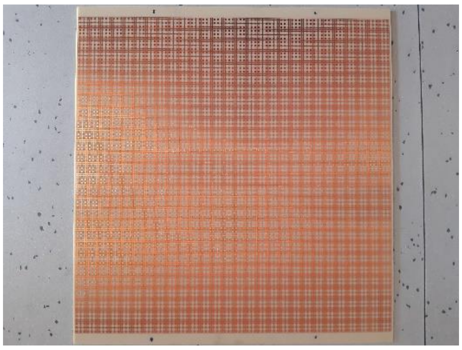

Fig. 10. PCB prototype.

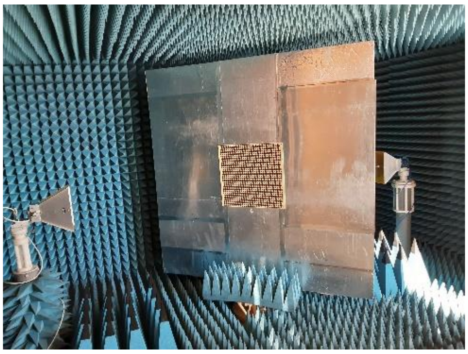

Fig. 11. Measurement setup.

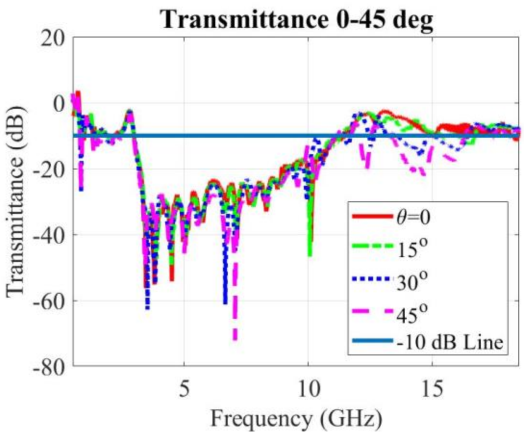

Fig. 12. Measured results of transmittance in oblique incidence of TE waves.

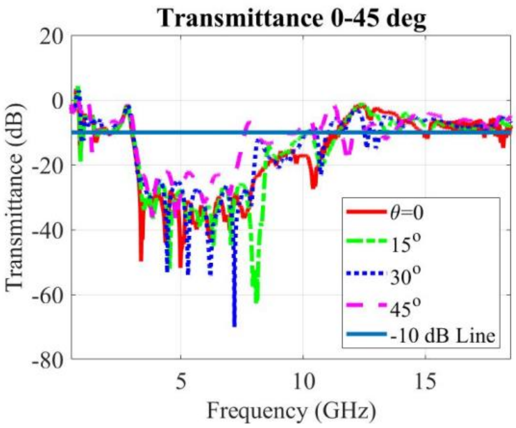

Fig. 13. Measured result of transmittance in oblique incidence of TM waves.

IV. CONCLUSIONS

An FSS acting as a band-stop spatial filter with a very large stopband, suitable for filtering in the UWB frequency range, has been proposed in this study, with good polarization insensitivity and angle stability. The structure was built using a budget friendly FR4 substrate.

Simultaneously, a very large stopband in the region of 1.78 and 14.32 GHz GHz was obtained. This compares favorably to other studies with similar objectives, such as [13], which reported a filtering band of 2.5-13.23 GHz, and [14], which reported a stopband of 3.1-13.3 GHz.

All two FSSs under consideration for comparison were implemented on FR4 substrates with a thickness of 1.6 mm. For our structure, parametric studies were conducted for substrate thickness and angular incidence.

To cover the UWB frequency range, tests for operation in oblique incidence were carried out, and angular insensitivities of 45° for both TE and TM waves were obtained. Simulation and measurement in an anechoic environment were used to evaluate the suggested structure. The collected results showed that theory and experimentation were in good agreement.

ACKNOWLEDGMENT

This work was supported by a grant of the Romanian Ministry of Research and Innovation, CCDI-UEFISCDI, project application number PN-III-P1-1.1-PD-2021-0010/within PNCDI III.

REFERENCES

[1] B.A.Munk, Frequency Selective Surfaces: Theory and Design. NewYork, NY, USA: Wiley, 2000.

[2] De Sabata, A.; Matekovits, L.; Buta, A.; Dassano, G.; Silaghi, A. Frequency Selective Surface for Ultra-Wide Band Filtering and Shielding. Sensors 2022, 22(5), 1896; https://doi.org/10.3390/s22051896.

[3] M. Kartal, J.J. Golezani, B. Doken, "A Triple Band Frequency Selective Surface Design for GSM Systems by Utilizing a Novel Synthetic Resonator", IEEE Trans. Antennas Propag., vol. 65, no. 5, pp. 2724-2727, May, 2017.

[4] S. Yadav, C.P. Jain, M.M. Sharma, " Smartphone Frequency Shielding With Penta-Bandstop FSS for Security and Electromagnetic Health Applications", IEEE Trans. Electromag. Compat., vol. 61, no. 3, pp. 887-892, June, 2019.

[5] W. Yin, H. Zhang, T. Zhong, X. Min, " A Novel Compact Dual-Band Frequency Selective Surface for GSM Shielding by Utilizing a 2.5-Dimensional Structure", IEEE Trans. Electromag. Compat., vol. 60, no. 6, pp. 2057-2060, Dec. 2018.

[6] M. Bashiri, C. Ghobadi, J. Nourinia, M. Majidzadeh, "WiMAX, WLAN, and X-Band Filtering Mechanism: Simple-Structured Triple-Band Frequency Selective Surface", IEEE Antennas Wireless Propag. Lett., vol. 16, pp. 3245-3248, 2017.

[7] U. Farooq, M.F. Shafique, M.J. Mughal, " Polarization Insensitive Dual Band Frequency Selective Surface for RF Shielding Through Glass Windows", IEEE Trans. Electromag. Compat., vol. 62, no. 1, pp. 93-100, June, 2020.

[8] S.B. Paiva, V.P. Silva Neto, A.G. D'Assunção, "A New Compact, Stable, and Dual-Band Active Frequency Selective Surface with Closely Spaced Resonances for Wireless Applications at 2.4 and 2.9 GHz", IEEE Trans. Electromag. Compat., vol. 62, no. 3, pp. 691-697, June, 2020.

[9] B. Döken, M. Kartal, " Easily Optimizable Dual-Band Frequency-Selective Surface Design", IEEE Antennas Wireless Propag. Lett., vol. 16, pp. 2979-2982, 2017.

[10] I.S. Syed, Y. Ranga, L. Matekovits, K.P. Esselle, S.G. Hay, "A Single-Layer Frequency-Selective Surface for Ultrawideband Electromagnetic Shielding", IEEE Trans. Electromag. Compat., vol. 56, no. 6, pp. 1404-1411, Dec. 2014.

[11] S. Ghosh, K.V. Srivastava, "Broadband Polarization-Insensitive Tunable Frequency Selective Surface for Wideband Shielding", IEEE Trans. Electromag. Compat., vol. 60, no. 1, pp. 166-172, Feb. 2018.

[12] A. Kocakaya, G, Çakir, "Novel angular-independent higher order band-stop frequency selective surface for X-band applications", IET Microw. Antennas Propag., vol. 12, no. 1, pp. 15-22, 2018.

[13] G.S. Paul, K. Mandal, "Polarization-Insensitive and Angularly Stable Compact Ultrawide Stop-Band Frequency Selective Surface", IEEE Antennas Wireless Propag. Lett., vol. 18, no. 9, pp. 1917-1921, Sept. 2019.

[14] S.S. Sampath, R. Sivasamy, "A Single-Layer UWB Frequency-Selective Surface With Band-Stop Response", IEEE Trans. Electromag. Compat., vol. 62, no. 1, pp. 276-279, Feb. 2020.

[15] CST Microwave Studio, Computer Simulation Technologies, v. 2021.

[16] L. Matekovits, A. De Sabata, and A. Silaghi, "Frequency Selective Surfaces with Two Quasi-Independent Notch Frequencies," IEEE Access, Vol.7, Issue 1, pp. 77261-77267, June 2019.